Earth's Future

RESEARCH ARTICLE
10.1029/2019EF001247

Future Hot and Dry Years Worsen Nile Basin Water Scarcity Despite Projected Precipitation Increases

Ethan D. Coffel[1,2,3], Bruce Keith[4], Corey Lesk[5,6], Radley M. Horton[5,6], Erica Bower[7], Jonathan Lee[8], and Justin S. Mankin[2,3,6]

[1]Neukom Institute, Dartmouth College, Hanover, NH, USA, [2]Department of Geography, Dartmouth College, Hanover, NH, USA, [3]Department of Earth Science, Dartmouth College, Hanover, NH, USA, [4]United States Military Academy—West Point, West Point, NY, USA, [5]Department of Earth and Environmental Sciences, Columbia University, New York, NY, USA, [6]Lamont Doherty Earth Observatory, Palisades, NY, USA, [7]United Nations, New York, NY, USA, [8]U.S. Army, Washington, DC, USA

Key Points:
- Poor crop yields are associated with hot and dry years in the Nile Basin
- Hot and dry years are projected to become more frequent, despite rising precipitation
- Increasing population coupled with hot and dry conditions will exacerbate water scarcity in the Nile Basin

Supporting Information:
- Supporting Information S1

Correspondence to:
E. D. Coffel,
ecoffel@dartmouth.edu

Citation:
Coffel, E. D., Keith, B., Lesk, C., Horton, R. M., Bower, E., Lee, J., & Mankin, J. S. (2019). Future hot and dry years worsen Nile Basin water scarcity despite projected precipitation increases. *Earth's Future*, *7*. https://doi.org/10.1029/2019EF001247

Received 1 MAY 2019
Accepted 31 JUL 2019
Accepted article online 5 AUG 2019

Abstract Compound extremes—particularly hot and dry years—can reduce crop yields and result in acute water scarcity. These risks are particularly pronounced in the Upper Nile Basin, a chronically water stressed agricultural region that includes western Ethiopia, South Sudan, and Uganda. While the causes of humanitarian crises in the Nile Basin are complex and involve governance, conflict, and climate, we demonstrate that nearly all recent regional crop failures have occurred amid hot and dry conditions and low runoff supplies. Using an observational ensemble, we find that such hot and dry years have been more frequent in recent decades, driven by increasing regional temperatures. This trend is likely to continue despite climate model projections of increasing regional precipitation. By the late 21st century, the frequency of hot and dry years may rise by a factor of 1.5–3, even if warming is limited to 2 °C. Regional water scarcity will continue to be a chronic issue for the Upper Nile from population growth alone, but runoff deficits during future hot and dry years will amplify this effect, leaving an additional 5–15% of the future population facing water scarcity. Climate change, along with the region's complex water politics, dependence on subsistence agriculture, and history of geopolitical instability, places the region at risk of severe food and water shortages as hot and dry years become more frequent. Adaptation and climate-resilient water management policies informed by an understanding of compound extremes will be essential to manage these risks.

Plain Language Summary The Upper Nile Basin covers parts of western Ethiopia, South Sudan, and Uganda and is at high risk of agricultural disruption due to climate extremes. Most agriculture in the region is rain fed, making yields vulnerable to hot and dry conditions. Recent droughts have severely reduced crop yields in the region, sometimes leading to food insecurity. This study shows that despite projected increases in regional precipitation due to climate change, the frequency of hot and dry years is likely to also rise due to warming. These increased hot and dry extremes will stress regional agriculture, and coupled with rapid population growth, they will exacerbate water scarcity across the Upper Nile Basin in the coming decades.

1. Introduction

The Upper Nile Basin covers parts of Ethiopia, South Sudan, and Uganda and is climatologically diverse, rapidly growing, and historically at risk for climate-induced agricultural shocks. Many inhabitants of the region are engaged in subsistence agriculture (African Union, Addis Ababa, n.d.), and there is strong evidence that heat and drought can damage crop yields, particularly when they co-occur (Kent et al., 2017; Lesk et al., 2016; Lobell et al., 2011; Matiu et al., 2017; Zscheischler et al., 2018; Figure 1). Climate extremes in the region—particularly hot and dry years—coupled with periodic water and food insecurity, as well as a history of geopolitical instability, can contribute to migration, conflict, and humanitarian disaster (Burrows & Kinney, 2016), as has occurred during a number of Upper Nile droughts in recent decades (Broad & Agrawala, 2000). By 2050, regional population is projected to more than double (World Population Prospects The 2012 Revision Volume I: Comprehensive Tables, 2013), imposing large additional demands on already-stressed ecosystems and likely complicating regional water politics (Asseng et al., 2018). As climate change raises temperatures and modifies precipitation patterns,

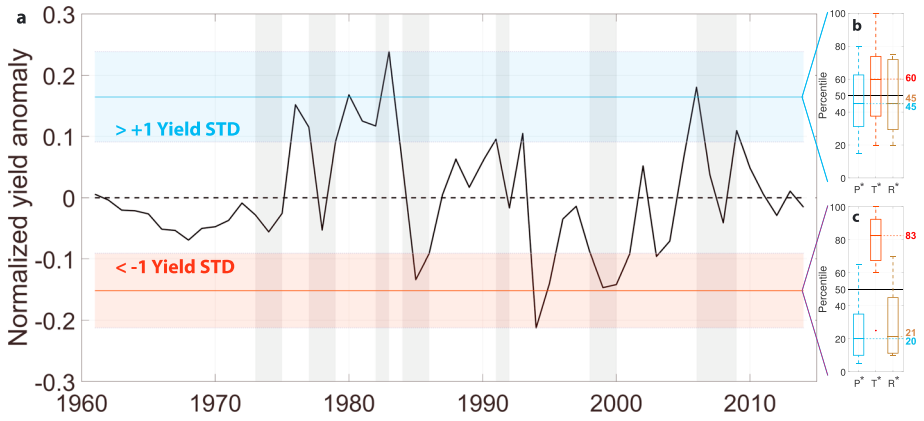

Figure 1. Poor crop yields co-occur with hot and dry years in Ethiopia. (a) Normalized, detrended yield anomalies averaged over six cereal crops (maize, millet, barley, pulses, sorghum, and wheat) in Ethiopia between 1961 and 2014, using UN Food and Agriculture data (black line; see section 2). Red (blue) shading indicates years with yield anomalies at least 1 standard deviation (STD) below (above) the mean. Gray vertical bars indicate years with armed conflict in Ethiopia (see section 2, and Table S1 for a list of armed conflicts). (b) Precipitation (*P*), temperature (*T*), and estimated runoff (*R*) percentiles in the 11 years with mean yields at least 1 STD above the mean (blue shading). (c) Precipitation, temperature, and estimated runoff percentiles in the 8 years with mean yields at least 1 STD below the mean (red shading). In (b) and (c), temperature and precipitation percentiles are calculated using the University of Delaware data set relative to a 1961–2000 baseline, and runoff percentiles are estimated using GLDAS (see section 2). Asterisks indicate that bootstrapped cumulative distribution function (CDFs) for precipitation, temperature, and runoff are significantly (K-S test, $p < 0.05$) different between years with good and poor yields (see Figure S4).

understanding the relationships among compound extremes, water supply, and its demand for food and human well-being will be critical to sustain development and avoid environmental and potentially humanitarian crisis in the region.

Nearly all of the rainfall that feeds the two major tributaries to the Nile—the Blue and White Nile—falls in South Sudan, western Ethiopia, and Uganda, with parts of the Lower Nile Basin—Sudan and Egypt—receiving very little precipitation and depending heavily on the Nile for water. The climate in the Upper Basin is strongly influenced by teleconnections with the El Niño–Southern Oscillation and with sea surface temperatures in the Indian Ocean and the Gulf of Guinea, which influence regional precipitation and thus Nile River streamflow (Giannini et al., 2003; Giannini et al., 2008; Kim & Kaluarachchi, 2009; Siam et al., 2014; Taye et al., 2011). Prior work has shown that global climate models project increases in annual mean rainfall and interannual precipitation variability (Siam & Eltahir, 2017), both of which have been linked to stronger and more frequent El Niño and La Niña events (Cai et al., 2014, 2015; Siam & Eltahir, 2017). As a result, the variability of Nile River streamflow could increase (Taye et al., 2011), requiring additional water storage capacity on the Nile and its tributaries to utilize and control the flow (Siam & Eltahir, 2017), while increasing the risk of both flooding and water shortage. Along with modified precipitation patterns, climate change will bring large increases in temperature across the region, raising the frequency, intensity, and duration of heat waves, as well as increasing evaporative demand on the soil and on the Nile River, its tributaries, and reservoirs.

2. Materials and Methods

2.1. Calculating Crop Yield Anomalies in Hot and Dry Years

We use annual yield data for maize, millet, barley, pulses, sorghum, and wheat from 1961–2014 in Ethiopia from the Food and Agriculture (FAO). These six crops represent the major staples of Ethiopia's food supply. Each crop's yield time series is normalized and detrended using two linear trends separated by a break point analysis to account for a sharp change in the growth rate of yields in the mid-2000s. For each crop listed above, the identified break points occur in 2006, 2009, 2006, 2006, 2007, and 2005, respectively. Finally, the detrended, normalized yields for each crop are averaged. Median temperature and precipitation percentiles during years with good (more than one standard deviation [STD] above the mean) and bad (more than

one STD below the mean) mean crop yields are identified using the University of Delaware data set relative to a 1961–2000 baseline (see supporting information).

2.2. Historical Trends and Future Projections of Hot and Dry Years in the Nile Basin

We assess historical climate trends in the Upper Nile Basin using eight observation-based data sets: the ERA-Interim reanalysis (1981–2016, temperature and precipitation), University of Delaware (1901–2016, temperature and precipitation), GLDAS version 2 (1961–2010, temperature and precipitation), CPC (1981–2016; temperature only), BerkeleyEarth (1901–2016, temperature only), HadCRUT4 (1901–2016, temperature only), GPCP (1981–2016; precipitation only), and CHIRPS-v2 (1981–2016; precipitation only). We compute linear trends from the time series of regionally and annually averaged monthly mean temperature and monthly total precipitation. Similarly, we compute historical temperature and precipitation trends across all available models (see Table S2) from the Coupled Model Intercomparison Project Phase 5 (CMIP5) models (variables: *tas* and *pr*) from 1981–2005 (using *r1i1p1* and the historical run). These model data are compared to an observational ensemble constructed using all temperature-precipitation combinations from the CPC, BerkeleyEarth, HadCRUT4, GPCP, and CHIRPS-v2 data sets. The longest available historical time series is used for each data set at the expense of comparing trends in time series of differing lengths.

Projected changes in temperature and precipitation are calculated in 2061–2085 as compared with 1961–2005 (to match the time period used in the historical crop yield analysis shown in Figure 1). Projections are made under Representative Concentration Pathway (RCP) 4.5 and RCP 8.5. Precipitation variability is computed for each model as the STD of annual mean precipitation with the linear trend removed. Detrending these precipitation data is necessary to avoid conflating changes in interannual variability with the long-term trend. All models are bilinearly regridded to a $2° \times 2°$ resolution to allow for spatial comparison. No bias correction is applied to the models, as each model's signal associated with future projections is compared to its historical simulations.

The Blue and White Nile Basins have different climatological distributions of rainfall and runoff yet share observed and projected climate trends that are similar in magnitude (Figures S5, S6, and S7). Because of their similar climate trends, we choose to aggregate our analysis across both basins.

We assess the changing frequency of hot and dry years in observations for three different thresholds of "hot" and "dry" to show the robustness of the observed increases in frequency across thresholds. We define hot and dry as those conditions consistent with years of poor agricultural yield: temperatures above the 83rd percentile and precipitation below the 20th percentile. For purposes of comparison, we employ two additional, more severe, definitions of hot and dry: temperature above the 85th and precipitation below the 15th and temperature above the 95th and precipitation below the 5th percentiles.

To assess the factors that drive projected increases in hot and dry years in the models, we use multivariate regression analysis. In order to increase the sample size and allow for a more robust estimate of coefficients, we relax our hot and dry thresholds to the be above the 50th percentile for temperature and below the 50th percentile for precipitation. Using these less strict hot and dry definitions, we estimate the contribution of changes in mean precipitation, precipitation variability, and their interaction to hot and dry years in 2020–2099 relative to the 1901–2005 distribution. Projected changes are computed for each model and each grid cell, and results for each model are normalized, allowing normalized regression coefficients to be computed across the CMIP5 model ensemble.

The chances of a year being hot and dry (with a temperature $\geq$83rd percentile and precipitation $\leq$20th percentile) absent temperature-precipitation correlation are calculated as (17/100) * (20/100). The factor by which temperature-precipitation correlation modifies the chances of a hot and dry year is calculated by dividing the observed frequency of hot and dry years by this expected frequency.

2.3. Assessing Changing Water Scarcity in the Nile Basin

Spatially explicit population projections consistent with the Shared Socioeconomic Pathways Project scenarios (Jones & O'Neill, 2016) are used to project future population growth. All projections are upscaled to $2° \times 2°$ resolution to match model projections. Only SSP scenarios consistent with each RCP are used (SSP3 and SSP5 for RCP 8.5 and SSP2 and SSP4 for RCP 4.5). Basin-wide runoff demand projections are

calculated for each decade by multiplying total population in that decade by water scarcity thresholds of 500, 1,000, and 1,700 m^3 per person per year (Gosling & Arnell, 2016). Runoff supply is computed from CMIP5 total runoff data (variable: mrro) by multiplying runoff in millimeters per day by each grid cell's area in square meters and subtracting the environmental flow requirement. Basin-wide runoff is calculated by summing over all grid cells in the Blue and White Nile Basins. This basin-wide aggregation likely reduces the runoff uncertainties due to parametrization of runoff and a lack of model representation of numerous other crucial runoff processes assuming the errors associated with them are normally distributed (Clark et al., 2015). The decadal mean runoff is computed for each model in each decade. While there is a projected upward trend in precipitation over the 21st century, this trend is slow enough not to result in significant changes indrologic modeling: 1. Modeling runoff over any particular 10-year period.

The percentage of the population with unmet runoff demand is computed by dividing projected runoff demand by projected runoff supply. Supply in hot and dry years is estimated for each model by selecting the years in each 21st century decade which are both hotter and drier than the decadal average. This definition differs from that in Figure 1c to allow for comparisons of runoff in hot and dry years in each decade; the number of years following the Figure 1c definition is too small to allow for such an analysis. Supply in normal years is estimated for each model by selecting all years in each 21st century decade which are not hot and dry.

The sensitivity of unmet runoff demand to the environmental flow requirement, water scarcity threshold, and the emissions scenario is estimated by varying each parameter while holding the others to their default values of a flow requirement of 60%, a 1,000-m^3-per-person-per-year scarcity threshold, RCP 8.5, and the mean of SSP3 and SSP5.

3. Results

3.1. Hot and Dry Years and Nile Agriculture

Understanding the climate conditions most impactful to the region, how such conditions will change in a warming world, and how they interact with social and political events is crucial to assessing future risk from environmental change. As shown in Figure 1, there are tight but complex linkages among climate, water availability, agricultural production, and regional stability. While strong evidence exists for the severely detrimental effects of heat and moisture shortage on crop yields on national or global scales (Lesk et al., 2016; Matiu et al., 2017), in regions such as the Nile Basin, the climatic contribution to negative agricultural shocks can be obscured by social, technological, and political events, as well as data constraints. To assess the effect of climate among these other critical factors, we conduct an analysis of the climate conditions present during years with poor yields in Ethiopia, which spans much of the Upper Nile Basin. Ethiopia is rare among Upper Nile countries in that it provides the long-term agricultural yield data against which we can assess the agricultural impacts of extreme climate conditions, such as hot and dry years.

Figure 1a shows that Ethiopian crop yields exhibit substantial interannual variability, resulting from interactions among climate (Figures 1b and 1c), governance, and war (gray vertical shading, Figure 1a, see Table S1), along with other environmental and social factors. Despite the varied sources of yield variability, we find consistently normal climate conditions in years with good crop yields (at least one STD above the mean), with median temperature, precipitation, and runoff at the 60th, 45th, and 45th percentiles, respectively (Figure 1b), suggesting that regional agricultural practices are potentially adapted to the average twentieth-century climate. Climate conditions are not significantly different during years with good crop yields as compared to years with normal crop yields (Figure S1). In contrast, years with poor yields are almost always both hot and dry with median temperature, precipitation, and runoff at the 20th, 83rd, and 21st percentiles, respectively (Figure 1c). These results are robust across individual crops (Figure S2) and detrending methods (Figure S3) and are statistically significant; similar percentile results are found for 1,000 bootstrapped yield time series (Figure S4). The similar climate conditions found in years with normal and above-normal yields suggests that in good years, nondamaging climate conditions combine with favorable nonclimatic factors (such as perhaps a lack of conflict or detrimental policy conditions) to promote higher agricultural output.

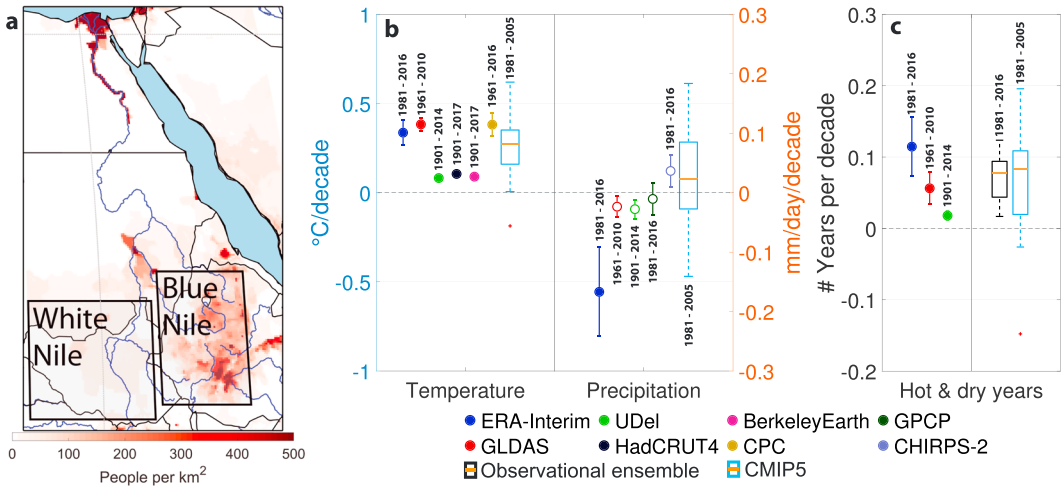

Figure 2. Historical trends in the Nile Basin. (a) The Upper Nile Basin, with the Blue and White Nile regions outlined. Red shading shows 2010 population density (see section 2). (b) Trends in annual mean temperature and precipitation in the combined Blue and White Nile region across eight observation-based data sets and the historical Coupled Model Intercomparison Project Phase 5 model ensemble. Boxplots show the range across 31 models, with the orange horizontal line indicating the multimodel median. (c) Trends in the frequency of hot and dry years (temperatures above the historical 83rd percentile and precipitation below the historical 20th percentile, see Figure 1c) in the combined Blue and White Nile region for three joint temperature-precipitation data sets, an ensemble of all combinations of observed temperature and precipitation data sets (see section 2), and the Coupled Model Intercomparison Project Phase 5 model ensemble. The time period for the data sets varies and is shown above each unique trend marker in (b) and (c). Filled circles indicate significant ($p < 0.05$) linear trends. Error bars show the standard error around trend coefficient estimates. In all boxplots, boxes represent the interquartile range, whiskers represent the 99.3rd and 0.7th percentiles, and red crosses represent outlier models beyond this range.

3.2. Hot and Dry Years in the Past and Future

Given this consistent co-occurrence of hot and dry conditions and poor agricultural yields in Ethiopia, we examine how such hot and dry conditions have changed over the historical record over the entirety of the Upper Nile Basin (Figure 2a), where agricultural conditions are similar and where much of the precipitation that feeds the Nile River falls. We divide the basin into two regions, roughly corresponding to the Blue and White Nile Basins, which we analyze together (see section 2). We employ five observed temperature data sets (ERA-Interim (Dee et al., 2011), University of Delaware (Willmott & Matsuura, 2018), CPC ("CPC Global Temperature Data,", n.d.), HadCRUT4 (Morice et al., 2012), and BerkeleyEarth), four observed precipitation data sets (ERA-Interim, University of Delaware, GPCP (Adler et al., 2003), and CHIRPS-2 (Funk et al., 2015)), and one land surface reanalysis data set (GLDAS (Matthew & Beaudoing, 2015), forced by Princeton meteorological forcing of temperature and precipitation), covering various time periods between 1901 and 2016. These data sets are compared with each other and with a suite of 31 models from CMIP5 (Taylor et al., 2012; see Table S1 for selected CMIP5 models and Figure S5 for model verification with historical data in the Nile Basin).

Temperatures show a consistent and statistically significant ($p < 0.05$) upward trend in all observation-based data sets, while the CMIP5 models show positive but not always significant trends (Figure 2b; left). Precipitation observations show nonsignificant and near-zero long-term trends in both models and observations (Figure 2b; right). Sparse regional precipitation measurements likely contribute to the disagreement about precipitation changes across observational products. The models generally show trends of comparable magnitude and direction as the observation-based data sets: Approximately two thirds of models have significant ($p < 0.05$; 22/31 models) positive temperature trends, while only 4/31 models have significant (positive) trends in precipitation. The distribution of modeled precipitation trends is not significantly different than the distribution of observed trends (K-S test, $p < 0.05$), leading us to conclude that the models are appropriate tools for the analysis herein.

Stationary precipitation coupled with rising temperatures have driven significant increases in the frequency of hot and dry years since 1901 (Figure 2c). We compare the distributions of trends in hot and dry years from three joint temperature-precipitation data sets (ERA-Interim, GLDAS, and UDel) with an ensemble of

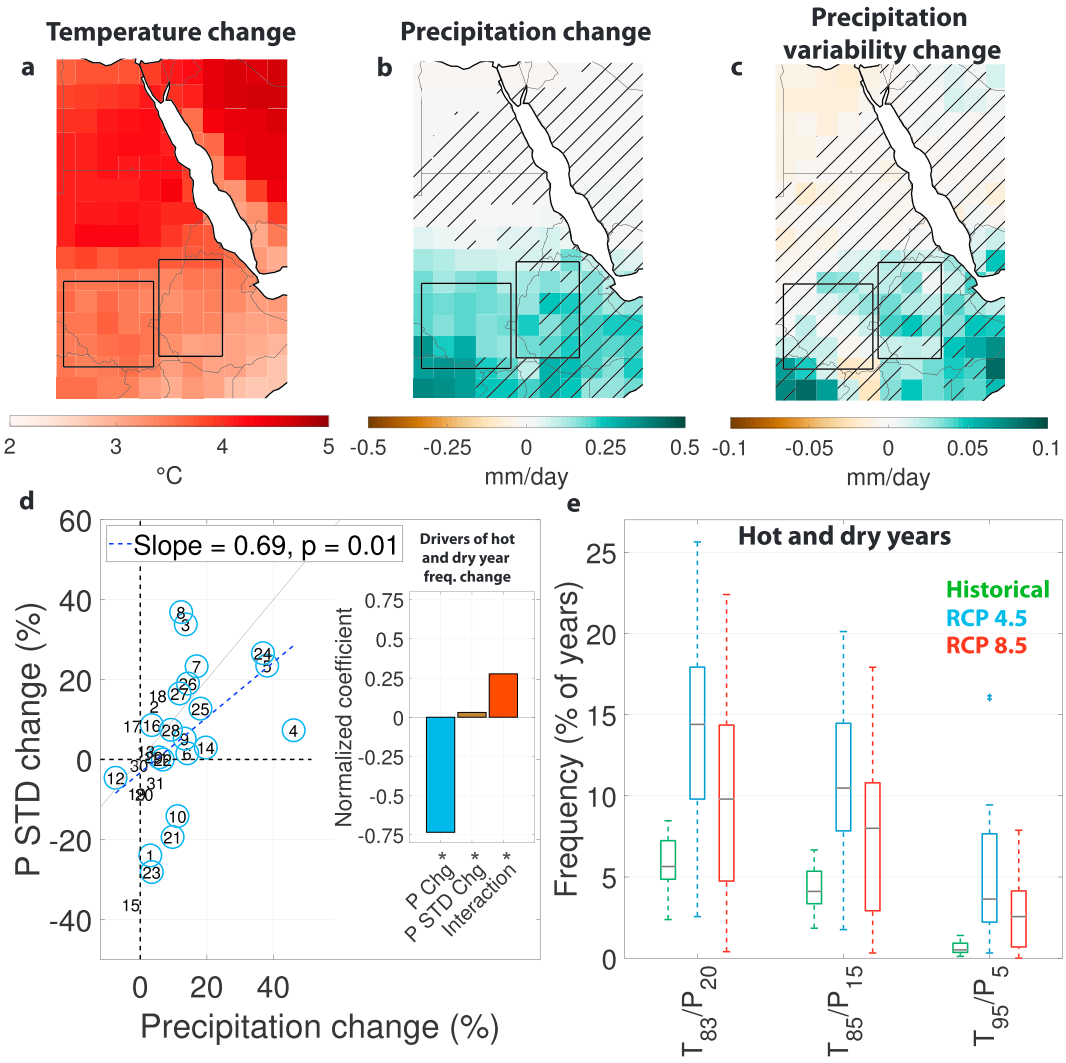

Figure 3. Future changes in temperature, precipitation, and the frequency of hot and dry years. Multimodel median projected change in annual mean temperature (a), precipitation (b), and the standard deviation of detrended annual mean precipitation (c) in 2061–2085 relative to 1961–2005 under the Representative Concentration Pathway (RCP) 8.5 emissions scenario, across the Coupled Model Intercomparison Project Phase 5 (CMIP5) model ensemble. Hatching indicates less than two-thirds model agreement on the direction of change. (d) Percentage change in precipitation (*P*) versus percentage change in interannual precipitation standard deviation (*P* STD) across the CMIP5 ensemble. Blue circles indicate models with significant (K-S test, $p < 0.05$) precipitation change. The blue dashed line shows the linear fit across models (slope = 0.69, $p = 0.01$). Gray line shows the 1:1 line. See Table S1 for a list of models. Inset shows relative contributions of precipitation change (*P* Chg), precipitation standard deviation change (*P* STD Chg), and their interaction to the change in hot and dry year frequency (see section 2). Asterisks in the inset box plot in (d) indicate significant regression coefficients ($p < 0.05$; e): Frequency of hot and dry years using differing definitions of hot and dry in the historical period (green), RCP 4.5 (blue), and RCP 8.5 (red). Boxplots show the range across the CMIP5 ensemble. Boxes represent the interquartile range, whiskers represent the 99.3rd and 0.7th percentiles, and red crosses represent outlier models beyond this range.

combinations of the three independent temperature (BerkeleyEarth, HadCRUT4, and CPC) and two independent precipitation (GPCP and CHIRPS-2) data sets shown in Figure 2b as well as with the CMIP5 ensemble. All observation-based temperature-precipitation data sets (ERA-Interim, GLDAS, and UDel) show upward, significant ($p < 0.05$) trends in the occurrence of hot and dry years in the Upper Nile over the record. In addition, the CMIP5 ensemble median generally agrees with the observational ensemble, indicating that the models have captured the range of observed trends in these extremes over recent decades.

The observed upward trends in hot and dry years are projected by all models to continue throughout the 21st century, driven by rapidly rising temperatures (Figure 3a) and slightly mitigated by modest increases in precipitation (Figure 3b). All models project mean temperature increases of 2–4 °C, while one half to two thirds of models project annual mean precipitation increases of 0.1–0.5 mm/day (0 to +10% change) by 2061–2085

as compared with 1961–2005 under RCP 8.5, with somewhat reduced changes under RCP 4.5 (see Figure S8). Alongside the increase in total precipitation, interannual precipitation variability (represented by the STD of detrended annual mean precipitation) is uncertain and projected to change from −30% to +40% across models, with a slight increase in the multimodel median (Figures 3c and 3d; see section 2). However, the magnitude of projected model changes in total precipitation are positively correlated with changes in interannual precipitation variability (Figure 3d; $r = 0.69$, $p = 0.01$). As a result, hot and dry years are more frequent across the ensemble than they would be absent this positive correlation: When controlling for total model-based precipitation change, this correlation results in larger increases in hot and dry year frequency (Figure 3d, inset) than would be expected if no relationship across the ensemble existed. Additionally, moderately strong annual temperature-precipitation correlations (−0.5 to −0.75) in the region increase the frequency of hot and dry years by a factor of 1.5–2.0 compared to a world where temperature and precipitation are uncorrelated (see section 2) in the historical period and will continue to do so in the future (see Figure S9). Temperature variability is not assessed, as due to mean warming most future dry years are projected to also be hot. Because of monotonic temperature increases, each year is projected to be hot by the models; coupled with an increase in precipitation variability (despite mean precipitation increases), the likelihood of a given year in the future being both hot and dry increases markedly (Diffenbaugh et al., 2015).

Because of their association with poor agricultural yields historically (Figure 1c), we know precipitation anomalies below the 20th percentile and temperature anomalies above the 83rd percentile (relative to 1961–2005) generate hot and dry years that are impactful to people in the Upper Nile. In total, the frequency of hot and dry years equivalent in magnitude to those associated with the historically poor crop yields is projected to increase by a median factor of 1.8 (range: 0.5–2.5) under RCP 8.5 and 2.6 (range: 0.9–3.4) under RCP 4.5. Historically, such conditions occurred in 6% of years; by 2061–2085, 14% and 10% of years are projected to experience the same or worse hot and dry conditions under RCP 4.5 and RCP 8.5, respectively (Figure 3e). Substantial increases in frequency are also projected for more extreme definitions of hot and dry years (Figure 3e; T_{85}/P_{15}: median factor of 2.0 [2.6], T_{95}/P_5: median factor of 5.2 [10.0], under RCP 8.5 [RCP 4.5]). We note that seven out of 31 models project the frequency of hot and dry years to stay the same or decline, suggesting that either low-frequency hydroclimate variability or model structure is a crucial source of uncertainty for these projections. However, the robust increase in basin precipitation projected with a large initial condition ensemble (Mankin et al., 2017) suggests that model structure may be a more important source of uncertainty for precipitation change than internal variability.

Interestingly, the increase in frequency of hot and dry years is slightly greater under the lower forcing of RCP 4.5 than the higher forcing of RCP 8.5 (Figure 3e). This counterintuitive result occurs because of the larger increase in mean precipitation projected under the higher RCP 8.5 emissions scenario and highlights how considering compound climate extremes (here hot and dry years) in some cases complicates the assumption that more warming monotonically increases climate risk. However, despite the modestly lower hot and dry year frequency under RCP 8.5, temperatures under the higher emissions scenario are more extreme; furthermore, these results suggest that the Upper Nile region is committed to facing increasing hot and dry years over the near-term decades regardless of mitigation choices.

3.3. Increasing Water Scarcity in the Nile Basin, Exacerbated by Hot and Dry Years

Yet climate conditions (such as hot and dry occurrence) are not the only, nor even the most important, factor determining future water stress. A rapidly rising population is likely to dramatically increase water stress in the Nile Basin as measured by per-capita runoff supply, irrespective of climate change and in spite of the projected increase in future precipitation (Figure 4). But the increasing frequency of hot and dry years projected by the CMIP5 ensemble amplifies the chronic water scarcity driven by this secular trend in population. We quantify the balance between runoff supply and demand under a variety of definitions of water scarcity, environmental flow requirements within the Nile Basin, and population trajectories to assess the factors driving projected increases in runoff deficits. Our projections conservatively assume that basin-wide runoff is equally available to the basin's population.

Projected multimodel median runoff supply (using a subset of 15 of the 31 CMIP5 models that provide runoff data; see Table S2 for a list of models and Figure S10 for a comparison of model projections using this subset and the full 31-member ensemble) does not substantially increase through 2080 (Figure 4a, blue and brown boxplots), due to the increased evaporative demand from higher temperatures counteracting the modest

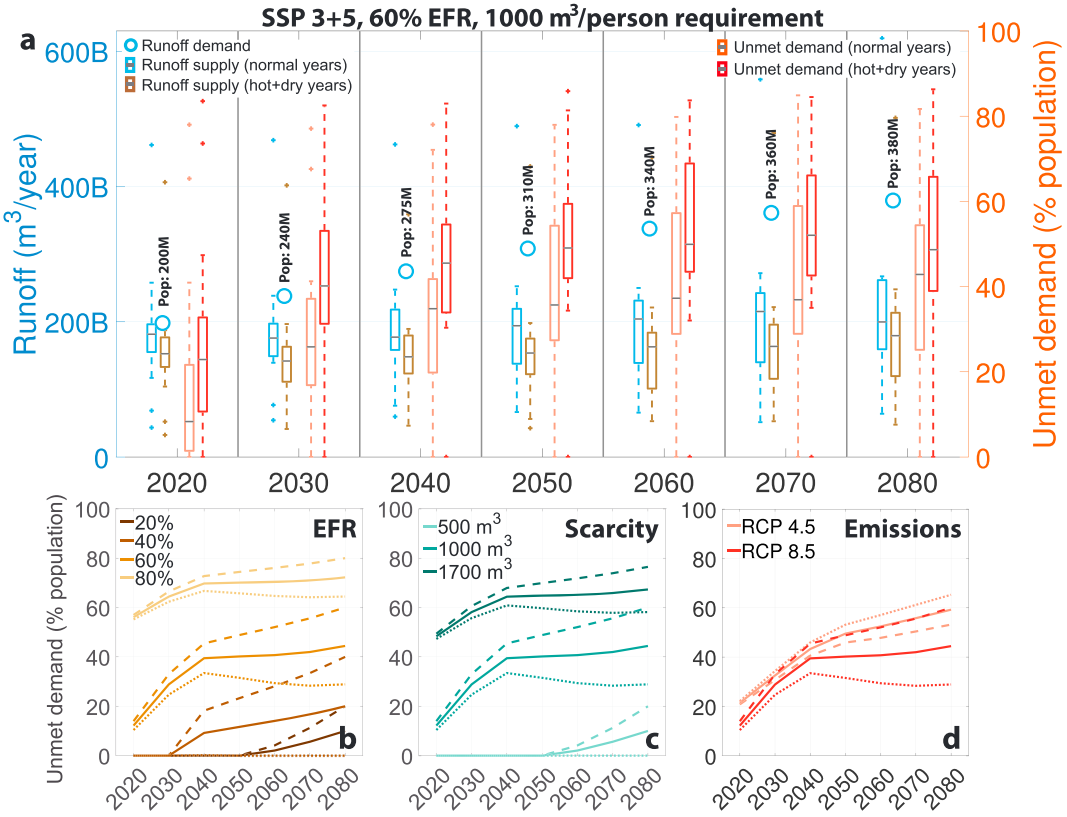

Figure 4. Increasing basin-wide water scarcity exacerbated by hot and dry years. (a) Projected changes in runoff supply during normal years (blue boxplots) and hot and dry years (brown boxplots), both assuming an environmental flow requirement (EFR) of 60% (see section 2) and Representative Concentration Pathway (RCP) 8.5. Blue circles indicate runoff demand, assuming historical per-capita usage, a water scarcity threshold of 1,000 m^3 per person per year, and population changes from an average of the SSP3 and SSP5 (Jones & O'Neill, 2016) scenarios (see section 2). The percentage of runoff demand which is unmet is shown in normal years (orange boxplots) and in hot and dry years (red boxplots; see section 2). (b) Water scarcity under differing environmental flow requirements and a scarcity threshold of 1,000 m^3 per person per year and RCP 8.5. (c) Water scarcity under differing per-capita thresholds and an environmental flow requirement of 60% and RCP 8.5. (d) Water scarcity under RCP 4.5 and RCP 8.5 with an environmental flow requirement of 60% and a scarcity threshold of 1,000 m^3 per person per year. In (b) and (c), runoff projections use RCP 8.5; solid lines show results with an average of the SSP3 and SSP5 population scenarios, dashed lines show SSP3, and dotted lines show SSP5. In (d) dashed and dotted lines for RCP 8.5 show results using SSP3 and SSP5, while dashed and dotted lines for RCP 4.5 show results using SSP2 and SSP4.

regional precipitation increases. However, runoff demand, assuming a conservative per-capita minimum water requirement of 1,000 m^3/year and an environmental flow requirement of 60%, approximately doubles from 200 billion cubic meters per year to 400 billion cubic meters per year as regional population increases following the mean of the SSP3 and SSP5 scenarios, both of which are compatible with RCP 8.5 (Jones & O'Neill, 2016; Figure 4a, blue circles). By 2030, estimated runoff demand almost always exceeds the projected multimodel median runoff supply and the percentage of the regional population for whom there is insufficient water rises sharply. By 2080, we estimate 95 to 250 million people per year (25–65% of regional population; Figure 4a, orange and red boxplots) could face chronic water scarcity (per-capita annual supply of <1,000 m^3), as compared to less than 25 million in 2020. We also note that most of this increase in unmet runoff demand occurs during a rapid rise between 2020 and 2040, concurrent with the lower forcing (and lower mean precipitation increase; see Figure 3e).

On top of this background rise in water scarcity, the increasing frequency of hot and dry years (Figure 3e; those both hotter and drier than the decadal mean; see section 2) will result in more negative shocks to runoff supply. We find that runoff supply is approximately 20% lower than normal during hot and dry years, a deficit that is projected to remain roughly constant through the 21st century (Figure 4a, blue and brown boxplots). Crucially, however, base level per-capita runoff supply will be lower in the future due to population increase, meaning that the runoff deficits in hot and dry years will result in large increases in the number of

people with unmet runoff demand as compared to normal years. On average in 2020–2090, we find that 20–40% (~10M in 2020 rising to ~170M by the 2080s) of the population may have unmet demand during normal years and 30–55% (~25M in 2020 rising to ~200M by the 2080s) during hot and dry years (Figure 4a), with these percentages generally being higher in later decades.

However, real-world environmental flow requirements are uncertain and depend on complex regional hydrology influenced by vegetation, terrain, and geopolitical factors (such as treaties governing the use of water from Nile tributaries). In addition, a variety of per-capita definitions of water scarcity exist, and trajectories of future population growth and greenhouse gas emissions are uncertain. To account for some of these uncertainties, we show the evolution of runoff supply deficits under three population growth scenarios for a variety of plausible environmental flow requirements (Figure 4b), water scarcity thresholds of 500 m^3 per person per year (absolute water scarcity), 1,000 m^3 per person per year (chronic water scarcity), and 1,700 m^3 per person per year (water stress; Gosling & Arnell, 2016; Figure 4c), and the RCP 4.5 and RCP 8.5 emissions scenarios (Figure 4d), holding other parameters to their default values as shown in Figure 4a (60% environmental flow requirement, 1,000-m^3 scarcity threshold, and RCP 8.5). We note that the environmental flow requirement is the largest contributor to unmet runoff demand uncertainty, followed by the population scenario, and finally the emissions scenario.

4. Conclusions

Populations in the Upper Nile Basin are highly vulnerable to climate extremes and their impacts, including crop failures driven by drought, floods, heat, and the spread of agricultural pests and vector-borne diseases. While the majority of climate models suggest hot and dry years will become more frequent, large-scale circulation biases or subgrid scale processes not well represented in the models could result in some regions being more or less water scarce than projected here in absence of changes in population and net water consumption. In addition, the CMIP5 models are known to perform poorly over other parts of East Africa, particularly in Somalia and Kenya (Rowell et al., 2015). However, our analysis suggests that the seasonal rainfall and temperature cycles in the Upper Nile Basin are relatively well represented by the CMIP5 ensemble, lending some confidence to these projections (Figure S5). Our results point to increasing regional water scarcity even in the face of increasing precipitation; if precipitation remains constant or declines in the future, hot and dry years will become more frequent than we project here.

As the Upper Nile Basin develops, additional multiyear water storage coupled with groundwater withdrawals and interbasin transfers may be able to provide additional water resources in some regions; though it is unclear whether such withdrawals would be sustainable (Gleeson et al., 2012). Finally, research is needed on how climate change alongside industrialization and modified agricultural practices will influence society in the region, to what extent climate extremes contribute to migration and conflict, and which adaptation strategies are most effective and efficient at reducing regional climate risk.

Our results demonstrate that hot and dry years have become more common over the past four decades in the Upper Nile Basin. This trend is projected to continue by nearly all CMIP5 models, despite uncertainty in model representations of ocean-atmosphere teleconnections, land-atmosphere feedbacks, and regional monsoon dynamics. Because of large population increases, water scarcity as measured by per-capita runoff deficits will likely increase and this scarcity will be exacerbated by hot and dry conditions. In addition, while trends in hot and dry year frequency are sensitive to uncertain projected precipitation changes, the strong dependence of per-capita runoff supply on population growth makes it unlikely that larger than expected precipitation increases would significantly improve water scarcity outcomes in the region over the near-term decades. Finally, the increasing frequency of hot and dry years will raise the likelihood of multiyear hot and dry spells, during which impacts on agriculture and people may compound nonlinearly. Our results highlight the need for regional development efforts to urgently focus on climate resilience as the Upper Nile Basin undergoes rapid climate and socioeconomic change in the coming decades.

Funding

Funding for this work was provided by the Dartmouth Neukom Institute.

Author Contributions

E. D. C., J. S. M., B. K., and C. L. conceived of the study. E. D. C. and J. S. M. designed the analysis. E. D. C. performed the analysis. E. D. C, J. S. M., B. K., and C. L. interpreted the results. E. D. C. and J. S. M. wrote the manuscript with contributions from B. K., C. L., R. M. H., E. B., and J. L.

Competing interests

The authors have no competing interests.

Data Availability

Raw CMIP5 data are freely available from the Earth System Grid Federation repositories at https://esgf-node.llnl.gov/projects/cmip5/. NOAA CPC is freely available at https://www.esrl.noaa.gov/psd/data/gridded/data.cpc.globaltemp.html. ERA-Interim reanalysis data are freely available at https://apps.ecmwf.int/datasets/data/interim-full-daily/levtype=sfc/. GPCP precipitation data are freely available at https://www.esrl.noaa.gov/psd/data/gridded/data.gpcp.html. CHIRPS-2 precipitation data are freely available at https://www.chc.ucsb.edu/data/chirps/. GLDAS data are freely available at https://disc.gsfc.nasa.gov/datasets?keywords=GLDAS. BerkeleyEarth temperature data are freely available at http://berkeleyearth.org/. HadCRUT4 temperature data are freely available at https://crudata.uea.ac.uk/cru/data/temperature/. University of Delaware temperature and precipitation data are freely available at https://www.esrl.noaa.gov/psd/data/gridded/data. UDel_AirT_Precip.html. FAO yield data are available freely online from FAOSTAT at http://www.fao.org/faostat/en/.

Acknowledgments
We acknowledge the World Climate Research Programme's Working Group on Coupled Modelling, which is responsible for CMIP, and we thank the climate modeling groups for producing and making available their model output. For CMIP the U.S. Department of Energy's Program for Climate Model Diagnosis and Intercomparison provides coordinating support and led development of software infrastructure in partnership with the Global Organization for Earth System Science Portals.

References

Adler, R. F., Huffman, G. J., Chang, A., Ferraro, R., Xie, P.-P., Janowiak, J., et al. (2003). The version-2 Global Precipitation Climatology Project (GPCP) monthly precipitation analysis (1979–present). *Journal of Hydrometeorology*, *4*(6), 1147–1167. https://doi.org/10.1175/1525-7541(2003)004<1147:TVGPCP>2.0.CO;2

Asseng, S., Kheir, A. M. S., Kassie, B. T., Hoogenboom, G., Abdelaal, A. I. N., Haman, D. Z., & Ruane, A. (2018). Can Egypt become self-sufficient in wheat? *Environmental Research Letters*, *13*(9). https://doi.org/10.1088/1748-9326/aada50

Broad, K., & Agrawala, S. (2000). CLIMATE: The Ethiopia food crisis—Uses and limits of climate forecasts. *Science*, *289*(5485), 1693–1694. https://doi.org/10.1126/science.289.5485.1693

Burrows, K., & Kinney, P. L. (2016). Exploring the climate change, migration and conflict nexus. *International Journal of Environmental Research and Public Health*, *13*(4), 443. https://doi.org/10.3390/ijerph13040443

Cai, W., Borlace, S., Lengaigne, M., van Rensch, P., Collins, M., Vecchi, G., et al. (2014). Increasing frequency of extreme El Niño events due to greenhouse warming. *Nature Climate Change*, *4*(2), 111–116. https://doi.org/10.1038/nclimate2100

Cai, W., Wang, G., Santoso, A., McPhaden, M. J., Wu, L., Jin, F.-F., et al. (2015). Increased frequency of extreme La Niña events under greenhouse warming. *Nature Climate Change*, *5*(2), 132–137. https://doi.org/10.1038/nclimate2492

Clark, M. P., Nijssen, B., Lundquist, J. D., Kavetski, D., Rupp, D. E., Woods, R. A., et al. (2015). A unified approach for process-based hydrologic modeling: 1. Modeling concept. *Water Resources Research*, *51*, 2498–2514. https://doi.org/10.1002/2015WR017198

CPC Global Temperature Data. (n.d.). Retrieved April 23, 2018, from https://www.esrl.noaa.gov/psd/

Dee, D. P., Uppala, S. M., Simmons, A. J., Berrisford, P., Poli, P., Kobayashi, S., et al. (2011). The ERA-Interim reanalysis: Configuration and performance of the data assimilation system. *Quarterly Journal of the Royal Meteorological Society*, *137*(656), 553–597. https://doi.org/10.1002/qj.828

Diffenbaugh, N. S., Swain, D. L., & Touma, D. (2015). Anthropogenic warming has increased drought risk in California. *Proceedings of the National Academy of Sciences*, *112*(13), 3931–3936. https://doi.org/10.1073/pnas.1422385112

Funk, C., Peterson, P., Landsfeld, M., Pedreros, D., Verdin, J., Shukla, S., et al. (2015). The climate hazards infrared precipitation with stations—A new environmental record for monitoring extremes. *Scientific Data*, *2*(1), 1–21. https://doi.org/10.1038/sdata.2015.66

Giannini, A., Saravanan, R., & Chang, P. (2003). Oceanic forcing of Sahel rainfall on interannual to interdecadal time scales. *Science*, *302*(5647), 1027–1030. https://doi.org/10.1126/science.1089357

Giannini, A., Biasutti, M., Held, I. M., & Sobel, A. H. (2008). A global perspective on African climate. *Climatic Change*, *90*(4), 359–383. https://doi.org/10.1007/s10584-008-9396-y

Gleeson, T., Wada, Y., Bierkens, M. F. P., & Van Beek, L. P. H. (2012). Water balance of global aquifers revealed by groundwater footprint. *Nature*, *488*(7410), 197–200. https://doi.org/10.1038/nature11295

Gosling, S. N., & Arnell, N. W. (2016). A global assessment of the impact of climate change on water scarcity. *Climatic Change*, *134*(3), 371–385. https://doi.org/10.1007/s10584-013-0853-x

Jones, B., & O'Neill, B. C. (2016). Spatially explicit global population scenarios consistent with the shared socioeconomic pathways. *Environmental Research Letters*, *11*(8). https://doi.org/10.1088/1748-9326/11/8/084003

Kent, C., Pope, E., Thompson, V., Lewis, K., Scaife, A. A., & Dunstone, N. (2017). Using climate model simulations to assess the current climate risk to maize production. *Environmental Research Letters*, *12*(5), 054012. https://doi.org/10.1088/1748-9326/aa6cb9

Kim, U., & Kaluarachchi, J. J. (2009). Climate change impacts on water resources in the Upper Blue Nile River Basin, Ethiopia. *Journal of the American Water Resources Association*, *45*(6), 1361–1378. https://doi.org/10.1111/j.1752-1688.2009.00369.x

Lesk, C., Rowhani, P., & Ramankutty, N. (2016). Influence of extreme weather disasters on global crop production. *Nature*, *529*(7584), 84–87. https://doi.org/10.1038/nature16467

Lobell, D. B., Bänziger, M., Magorokosho, C., & Vivek, B. (2011). Nonlinear heat effects on African maize as evidenced by historical yield trials. *Nature Climate Change*, *1*(1), 42–45. https://doi.org/10.1038/nclimate1043

Mankin, J. S., Viviroli, D., Mekonnen, M. M., Hoekstra, A. Y., Horton, R. M., Smerdon, J. E., & Diffenbaugh, N. S. (2017). Influence of internal variability on population exposure to hydroclimatic changes. *Environmental Research Letters*, *12*(4), 044007. https://doi.org/10.1088/1748-9326/aa5efc

Matiu, M., Ankerst, D. P., & Menzel, A. (2017). Interactions between temperature and drought in global and regional crop yield variability during 1961-2014. *PLoS One*, *12*(5), e0178339. https://doi.org/10.1371/journal.pone.0178339

Matthew R., & Beaudoing, H. K. (2015). GLDAS Noah Land Surface Model L4 monthly 0.25 × 0.25 degree V2.0. Greenbelt, Maryland, USA.

Morice, C. P., Kennedy, J. J., Rayner, N. A., & Jones, P. D. (2012). Quantifying uncertainties in global and regional temperature change using an ensemble of observational estimates: The HadCRUT4 data set. *Journal of Geophysical Research*, *117*, D08101. https://doi.org/10.1029/2011JD017187

Rowell, D. P., Booth, B. B. B., Nicholson, S. E., & Good, P. (2015). Reconciling past and future rainfall trends over East Africa. *Journal of Climate*, *28*(24), 9768–9788. https://doi.org/10.1175/JCLI-D-15-0140.1

Siam, M. S., & Eltahir, E. A. B. (2017). Climate change enhances interannual variability of the Nile river flow. *Nature Climate Change*, *7*(5), 350–354. https://doi.org/10.1038/nclimate3273

Siam, M. S., Wang, G., Demory, M.-E., & Eltahir, E. A. B. (2014). Role of the Indian Ocean sea surface temperature in shaping the natural variability in the flow of Nile River. *Climate Dynamics*, *43*(3–4), 1011–1023. https://doi.org/10.1007/s00382-014-2132-6

Taye, M. T., Ntegeka, V., Ogiramoi, N. P., & Willems, P. (2011). Assessment of climate change impact on hydrological extremes in two source regions of the Nile River Basin. *Hydrology and Earth System Sciences*, *15*(1), 209–222. https://doi.org/10.5194/hess-15-209-2011

Taylor, K. E., Stouffer, R. J., & Meehl, G. A. (2012). An overview of CMIP5 and the experiment design. *Bulletin of the American Meteorological Society*, *93*(4), 485–498. https://doi.org/10.1175/BAMS-D-11-00094.1

African Union, Addis Ababa (n.d.). African Union Food Security.

Willmott, C. J., & Matsuura, K. (2018). Terrestrial air temperature and precipitation: Monthly and annual time series (1901-2017). Retrieved from http://climate.geog.udel.edu/~climate/html_pages/download.html

World Population Prospects The 2012 Revision Volume I: Comprehensive Tables, (2013) (Vol. 1). United Nations Population Division. https://doi.org/ST/ESA/SER.A/336

Zscheischler, J., Westra, S., van den Hurk, B. J. J. M., Seneviratne, S. I., Ward, P. J., Pitman, A., et al. (2018). Future climate risk from compound events. *Nature Climate Change*, *8*(6), 469–477. https://doi.org/10.1038/s41558-018-0156-3